Aircraft Supersonic Inlet with Dual Control System

ALEXANDRU NICOLAE TUDOSIE
Avionics Department, Faculty of Electrical Engineering
University of Craiova
105-107 Decebal Blvd., Craiova, Dolj
ROMANIA
atudosie@elth.ucv.ro, http://www.elth.ucv.ro,

JENICA ILEANA CORCAU
Avionics Department, Faculty of Electrical Engineering
University of Craiova
105-107 Decebal Blvd., Craiova, Dolj
ROMANIA
jcorcau@elth.ucv.ro, http://www.elth.ucv.ro,

Abstract: -The paper deals with an aircraft supersonic inlet with mixed compression, which has a dual control system, based on the inner total pressure's ratio preservation. The authors have identified the inlet's gas-dynamic behavior, as well as the main control and controlled parameters. One has also built the system's mathematical model, based on system's non-linear motion equations; furthermore, one has established, based on some simplifying hypothesis, the system's linear non-dimensional model, useful for further studies, as well as for some similar inlets' modeling. A system description based on block diagram with transfer functions was also realized. Some simulations were also performed, concerning the system's time behavior (step response), for different cases of control possibilities.

Key-Words: Supersonic, Inlet, Speed, Flow rate, Control, Shock wave, Pressure ratio, Flap.

1. Introduction

Supersonic inlets for the jet engines of modern supersonic aircraft are built in a large range of performances and types.

Supersonic air inlets with mixed (external and internal) compression have two different zones: a) the external zone, where the spike (or the wedge) generates a system of conic (oblique) shockwaves; b) the internal (inner) zone (the flow channel), profiled as a Laval nozzle. Both supersonic inlets, with mixed compression and with inner supersonic buffer zone, have an inner normal shock wave (developed in the divergent zone of the inlet's channel, behind the minimum section area zone), which position is determined by the flight regime (through the amount of the total pressure after the outer shock waves) and by the engine's operating regime (through the amount of the static pressure p_1 in the front of the engine's compressor). The flight regime consists of: the flight altitude H and

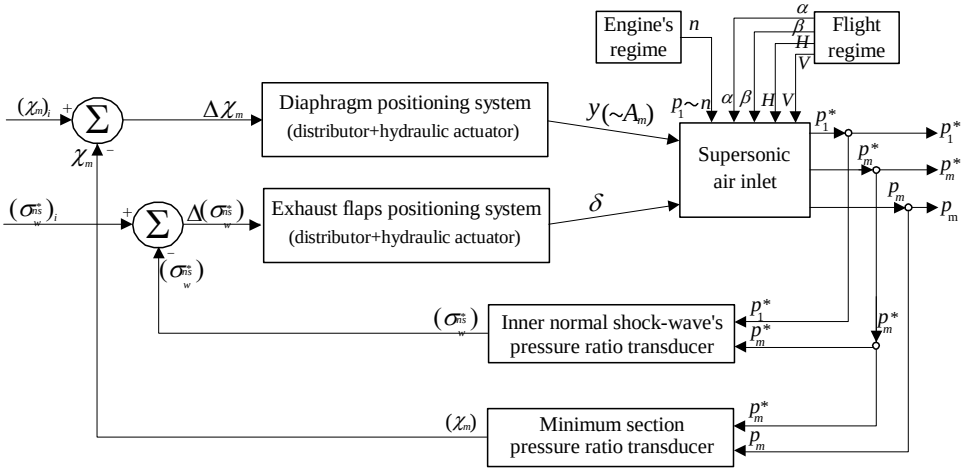

Fig. 1. Supersonic air inlet control system block-diagram

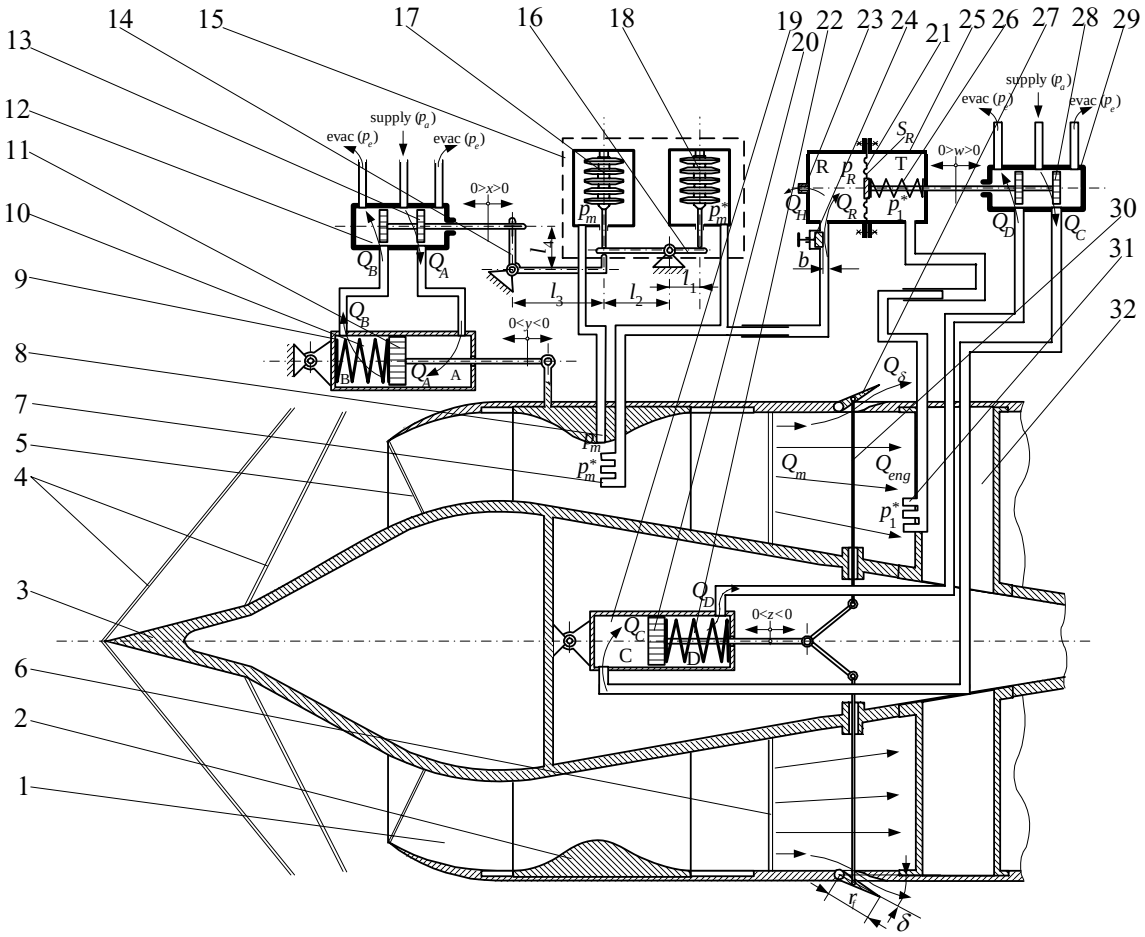

Fig. 2. Supersonic air inlet scheme

1-air intake; 2-diaphragm (inner cowl); 3-spike; 4- spike's shock waves; 5-intake's edge shock wave; 6-inner normal shock wave; 7-total pressure sensor's intake; 8-static pressure sensor's intake; 9-diaphragm's actuator; 10-spring; 11-actuator's piston; 12-distributor; 13-distributor's slide valve; 14-rocking lever; 15-pressure sensor; 16, 17-aneroid capsules; 18-sensor's lever; 19-exhaust flaps' actuators; 20-piston; 21-actuator's spring; 22-pressure ratio sensor; 23-drossel; 24-adjustable fluidic resistance; 25-elasic membrane; 26- sensor spring; 27-exhaust flap; 28-distributor; 29-slide valve; 30- exhaust flaps twin rods; 31-inlet's rear total pressure intake; 32-inlet's beam(s).

the flight speed *V*, both combined giving the Mach number M_H, respectively the aircraft (airplane) flight angles (which are the attack angle α and the sideslip angle β).

The possibilities of the inlet's control, in order to assure the balance of the engine's necessary air flow rate and the inlet's delivered air flow rate, are: a) the flow section area's control through the spike's positioning or through the intake's cowl's positioning; b) the inner minimum cross-section area control by the inner (cowl) diaphragm positioning; c) the inner normal shock wave's position control, through the exhaust flaps' opening control; d) combined methods.

Figure no.1 presents a formal block diagram of a supersonic air inlet with complex (dual) control system. The inlet control is realized by two (apparently independent) control systems: one for the minimum section position, the other for the normal shock wave positioning, their common part being the total pressure intake p_m^* .

The controlled parameters should be the inner normal shock wave's total pressure ratio σ_{nsw}^* (also known as "inlet's inner perfection co-efficient"), as well as the minimum section pressure ratio σ_m^* (or χ_m). One can observe that the system assures the internal pressure ratio's preservation through the inner cowl positioning as well as through the exhaust flaps' opening (both control systems being based on the feed back error's canceling).

System's constructive and operational diagram (containing also the main parts identifying) is depicted in fig. 2.

2. Inlet's Gas-Dynamic Behavior

The inlet in fig. 2 has a spike with two disturbance surfaces, which are generating two conic shock waves, so the inner airflow, inside the intake, remains supersonic. The airflow's speed is decreasing, until the sound speed is reached where the cross-section area has the minimum value (that means the critical section "*m*"), so the inner flow after this section should switch into subsonic.

Although, the real situation is a little different, the leap supersonic/subsonic being realized by a normal shock wave in the divergent side of the intake, so the flow in the minimum section remains supersonic; the minimum section becomes not the critical section, being over-dimensioned. This is the way to assure the gas-dynamic stability against any flow disturbances and also the inlet's "activation" during the transonic flights.

2.1. Inlet's Gas-Dynamic Properties

The inlet's perfection co-efficient σ_{DA}^{*} can be expressed as

$$\sigma_{DA}^{*} = \sigma_{csw1}^{*}\sigma_{csw2}^{*}\sigma_{m}^{*}\sigma_{nsw}^{*}\sigma_{f}^{*}, \qquad (1)$$

where $\sigma_{csw1}^{*}, \sigma_{csw2}^{*}$ = total pressure ratio for the two external conic shock waves generated by the spike, σ_{nsw}^{*} = total pressure ratio for the inner normal shock wave, σ_{f}^{*} = total pressure ratio (loss) because of the flow's friction, assumed as constant, respectively σ_{m}^{*} = minimum section pressure ratio; in fact, σ_{m}^{*} is equal to 1 if the normal shock wave is located at the inner channel minimum section (if the flow's Mach number is equal to 1) and decreases when it moves toward the compressor. σ_{m}^{*}-value is difficult to be measured by usual means, but it can be estimated using the flow's Mach number M_m, also estimated by the pressure ratio χ_m defined as

$$\chi_m = \frac{p_m}{p_m^{*}} = \left(1 + \frac{k-1}{2} M_m^{2}\right)^{\frac{k}{1-k}}, \qquad (2)$$

p_m^{*} – total pressure, p_m – static pressure measured at the inlet's channel minimum section „*m*", as Fig. 2 shows.

One can affirm that the terms $\sigma_{csw1}^{*}, \sigma_{csw2}^{*}$, $\left(\sigma_{csw1}^{*}\sigma_{csw2}^{*} = \sigma_{ext}^{*}\right)$, are depending on the flight regime (altitude *H*, speed *V*, attack angle α, sideslip angle β), σ_{nsw}^{*} is depending on the engine's regime (speed *n*), respectively σ_{m}^{*} and χ_m

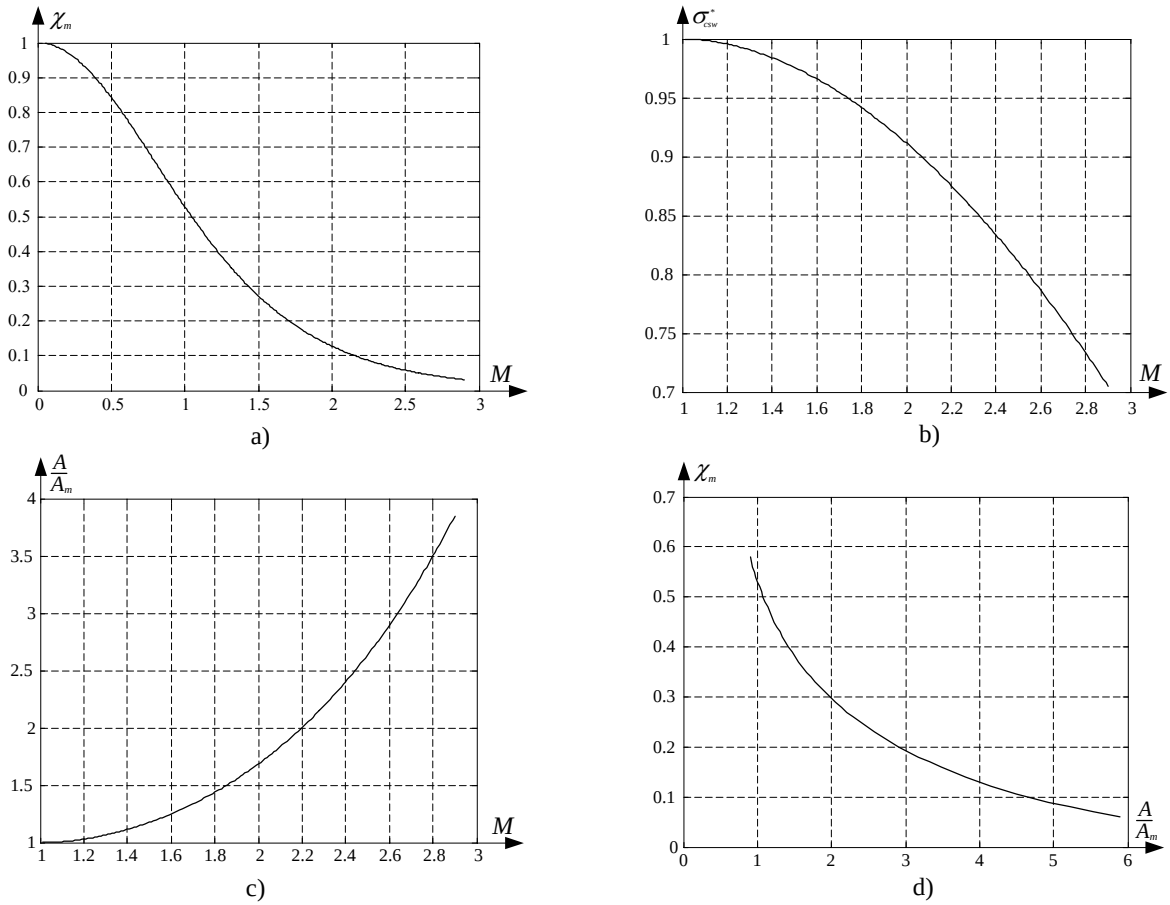

Fig. 3 Supersonic inlet's gas-dynamic characteristics

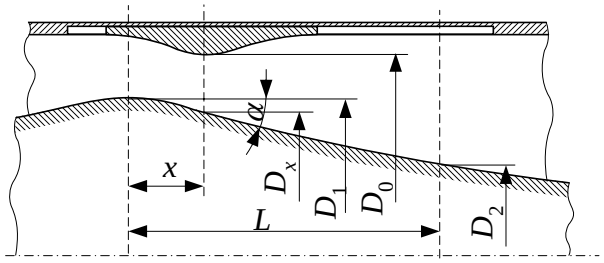

Fig. 4. Inlet inner channel geometry

on the flow's Mach number, as well as on the minimum section's area A_m, as shown in fig.3.

The mobile diaphragm assures the re-positioning of the minimum cross-section along the intake's inner channel, as well as its value modifying, (see fig. 4); the A_m current value is given by its position *x* inside the intake, as follows

$$A_m(x) = \frac{\pi}{L^2}\left\{4L^2\left(D_0^2 - D_2^2\right) + 4LD_2\left(D_2 - D_1\right)x - \right.$$
$$\left. - \left(D_2 - D_1\right)^2 x^2\right\}. \qquad (3)$$

2.2. Inner Normal Shock Wave Positioning

The inner normal shock-wave's position is determined by some gas-dynamic conditions, which can be reduced to only two elements: the total pressure in the inlet's channel before the normal shock wave, respectively the static pressure after the inlet's channel, in the front of the engine's compressor (as fig. 5 shows). Usually, the supersonic aircraft have axial-type compressors, which need a large amount of airflow rates and high entrance air speeds. The main parameter, which gives information about the engine's regime, is its rotation speed *n*. Fig. 5 shows the pressure's behavior during the flow through the inlet's channel, with respect to the p_1 pressure values and with the normal shock wave's position (section A, B, *x*, or the inlet's end).

The shock-wave's positioning, as well as its total pressure ratio, could be determined if one knows the thermo-dynamic parameters in section "*m*" as well as the pressure p_1 in the front of the compressor [6, 9], which is related to its rotation speed. Assuming as known the inlet's geometry, one can establish the dependence form for the inlet's section surface with respect to the current co-ordinate *x*, measured from the "*m*"-section; one can assume, close enough, a linear dependence:

$$A(x) = A_m + \frac{(A_1 - A_m)}{L}, \qquad (4)$$

where A_m, A_1 are the inlet's channel's extreme sections surfaces, *L*-inlet's channel length, *x*-

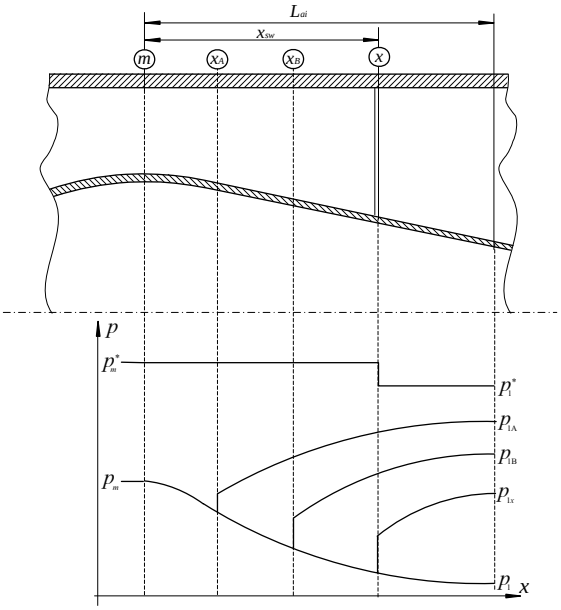

Fig. 5. Inner normal shock wave's positioning and the static and total pressure's variation

current co-ordinate, *A*(*x*)-current section's surface (fig. 5).

The formula for the air flow rate Q_a in section *x*,

$$Q_a(x) = KA(x)\frac{p^*}{\sqrt{T^*}}q(\lambda_x), \qquad (5)$$

(with $K = \sqrt{\frac{k}{R}\left(\frac{2}{k+1}\right)^{\frac{k+1}{k-1}}}$ =constant value, *R*- air specific constant, *k*-polytropic exponent, $q(\lambda_x)$– non-dimensional density, λ_x-speed co-efficient), can be applied for each important section (*m*, 1, before and after the shock-wave), resulting the row of equalities:

$$KA_m\frac{p_m^*}{\sqrt{T^*}}q(\lambda_m) = KA_x\frac{p_m^*}{\sqrt{T^*}}q(\lambda_{xb}) =$$
$$= KA_x\frac{p_m^*}{\sqrt{T^*}}q(\lambda_{xa}) = KA_1\frac{p_m^*}{\sqrt{T^*}}q(\lambda_1) \qquad (6)$$

which becomes, after simplifying,

$$\frac{q(\lambda_1)}{\Pi(\lambda_1)} = \frac{p_m^*}{p_1}q(\lambda_m)\frac{A_m}{A_1}, \qquad (7)$$

where $q(\lambda) = \lambda\left[\frac{k+1}{2}\left(1 - \frac{k-1}{k+1}\lambda^2\right)\right]^{\frac{1}{k-1}}$;

$$\Pi(\lambda) = \left(1 - \frac{k-1}{k+1}\lambda^2\right)^{\frac{k}{k-1}}. \qquad (8)$$

It results a transcendent equation, which argument is λ_1 and which has two roots, a supersonic one

($\lambda_1 > 1$) and a subsonic one ($\lambda_1 < 1$). The appropriate solution is the second one.

From Eq.(6) it also results, for the normal shock-wave, the total pressure ratio

$$\sigma^*_{nsw} = \frac{p_1^*}{p_m^*} = \frac{A_m}{A_1}\frac{q(\lambda_m)}{q(\lambda_1)}, \quad \sigma^*_{nsw} = \frac{q(\lambda_{xb})}{q\left(\frac{1}{\lambda_{xb}}\right)}, \quad (9)$$

which leads to a supersonic solution λ_{xb}, $(\lambda_{xb} > 1)$, for the second transcendent equation (9) and, also, to the expression for the normal shock-wave section area

$$A_x = A_1 \frac{q(\lambda_m)}{q(\lambda_{xb})}. \quad (10)$$

Once known the A_x value, it results, from Eq. (4), the shock wave's position

$$x_{sw} = \frac{LA_m}{A_1 - A_m}\left[\frac{q(\lambda_m)}{q(\lambda_{xb})}\right]. \quad (11)$$

So, one has obtained the shock wave's positioning, its total pressure ratio and a direct relation between this two parameters and the p_1 pressure.

The pressure in section 1 can be controlled through the exhaust flaps opening control (in order to eliminate the air flow excess).

3. System's Mathematical Model

The system's mathematical model consists of the motion equations for its main parts, for both of the above-mentioned sub-systems (as presented in [14] and [15]). All those equations are non-linear and need to be brought to an accessible form in order to be studied.

3.1. Non-linear Equation Systems

3.1.1. Diaphragm's Positioning System

a) inlet gas-dynamic properties (see fig. 3)

$$p_m^* = p_m^*(M_H, \alpha, \beta), \quad (12)$$

b) pressure ratio's transducer's equation:

$$S_{a1} l_1 p_m^* - S_{a2} l_2 p_m - \frac{l_2 l_4}{l_3}\left(m\frac{\mathrm{d}^2 x}{\mathrm{d}t^2} + \xi\frac{\mathrm{d}x}{\mathrm{d}t}\right) - \left(k_{r1} l_1 + k_{r2} l_2\right)x = 0, \quad (13)$$

where k_{r1}, k_{r2} – transducer's capsule's elastic constants; m – mobile rod and accessories mass; ξ – viscous friction co-efficient; l_1, l_2 – transducer's lever arms length; l_3, l_4 – transducer's rocking lever arms length; S_{a1}, S_{a2} – aneroid capsules surface areas (usually considered as equal $S_{a1} = S_{a2} = S_a$); x – distributor's slide-valve's displacement;

c) actuator's and distributor's equations:

$$Q_A = \mu_a L_d x\sqrt{\frac{2}{\rho_{hf}}}\sqrt{p_a - p_A}, \quad (14)$$

$$Q_B = \mu_a L_d x\sqrt{\frac{2}{\rho_{hf}}}\sqrt{p_B - p_e}, \quad (15)$$

$$Q_A = S_p\frac{\mathrm{d}(y_r - y)}{\mathrm{d}t} + \beta_{hf} V_{A0}\frac{\mathrm{d}p_A}{\mathrm{d}t}, \quad (16)$$

$$-Q_B = S_p\frac{\mathrm{d}(y + y_r)}{\mathrm{d}t} + \beta_{hf} V_{B0}\frac{\mathrm{d}p_B}{\mathrm{d}t}, \quad (17)$$

$$S_p(p_A - p_B) = m_p\frac{\mathrm{d}^2(y + y_r)}{\mathrm{d}t^2} + \xi_f\frac{\mathrm{d}(y + y_r)}{\mathrm{d}t} + k_{ea}(y_r + y + y_0), \quad (18)$$

where Q_A, Q_B – hydraulic fluid's flow rates; μ_a – flow rate co-efficient; L_d – distributor's orifice's width; p_A, p_B – actuator's chambers' pressures; y – actuator's rod's displacement; V_A, V_B – transducer's chambers volume; β_{hf} – hydraulic fluid's compressibility co-efficient; k_{ea} – actuator's spring's elastic constant; m_p – actuator's mobile rod and accessories mass; ξ_f – viscous friction co-efficient; p_a – hydraulic fluid supplying pressure; p_e – fluid's evacuation pressure (considered neglectable, because of its small value, comparing to p_A and p_B).

3.1.2. Exhaust Flaps' Positioning System

a) pressure ratio's transducer's equations:

$$Q_R = \mu_m b L_m\sqrt{\frac{2}{\rho_a}}\sqrt{p_m^* - p_R}, \quad (19)$$

$$Q_H = \mu_{dr}\frac{\pi d_{23}^2}{4}\sqrt{\frac{2}{\rho_a}}\sqrt{p_R}, \quad (20)$$

$$Q_R - Q_H = S_R\frac{\mathrm{d}w}{\mathrm{d}t} + \beta_{hf} V_R\frac{\mathrm{d}p_R}{\mathrm{d}t}, \quad (21)$$

$$S_R(p_R - p_1^*) = m_s\frac{\mathrm{d}^2 w}{\mathrm{d}t^2} + \xi_f\frac{\mathrm{d}w}{\mathrm{d}t} + k_1(w_r + w), \quad (22)$$

where Q_R, Q_H – airflow rate through the transducer's A chamber; μ_m, μ_{dr} – flow rate co-efficient; ρ_a – air's density; b, L_m- variable fluidic resistance's dimensions; d_{23} – transducer drossel

(23) diameter; S_R-transducer's elastic membrane's surface; V_R – R-chamber's volume; β_a – air's compressibility co-efficient; k_1 – transducer's spring's elastic constant; m_s – transducer's mobile rod and accessories mass; w – transducer's rod displacement;

b) actuator's and distributor's equations:

$$Q_C = \mu_a L_d x \sqrt{\frac{2}{\rho_{hf}}} \sqrt{p_a - p_C}\,, \tag{23}$$

$$Q_D = \mu_a L_d x \sqrt{\frac{2}{\rho_{hf}}} \sqrt{p_D - p_e}\,, \tag{24}$$

$$Q_C = S_a \frac{\mathrm{d}(z_r - z)}{\mathrm{d}t} + \beta_{hf} V_C \frac{\mathrm{d}p_C}{\mathrm{d}t}\,, \tag{25}$$

$$-Q_D = S_a \frac{\mathrm{d}(z + z_r)}{\mathrm{d}t} + \beta_{hf} V_D \frac{\mathrm{d}p_D}{\mathrm{d}t}\,, \tag{26}$$

$$S_a (p_C - p_D) = m_{ra} \frac{\mathrm{d}^2(z + z_r)}{\mathrm{d}t^2} + \xi_f \frac{\mathrm{d}(z + z_r)}{\mathrm{d}t} + k_2 (z_r + z + z_0), \tag{27}$$

where Q_C, Q_D – hydraulic fluid's flow rates; μ_a – flow rate co-efficient; L_d – distributor's orifice's width; p_C, p_D – actuator's chambers' pressures; z – actuator's rod's displacement; V_C, V_D – transducer's chambers volume; β_{hf} – hydraulic fluid's compressibility co-efficient; k_2 – actuator's spring's elastic constant; m_{ra} – actuator's mobile rod and accessories mass; ξ_f – viscous friction co-efficient; S_a – actuator's piston surface area.

c) inner channel pressure equations

$$p_1^* = p_1^*(n), \tag{28}$$

$$Q_m = Q_{ef} + Q_{eng}\,, \tag{29}$$

where Q_m – airflow rate through the minimum cross-section, Q_{ef} – airflow rate through the exhaust flaps opening, Q_{eng} – engine's necessary airflow rate,

$$Q_m = KA_m \frac{p_m^*}{\sqrt{T^*}} q(\lambda_m)\,, \tag{30}$$

$$Q_{ef} = \mu_f l_f r_f \delta \sqrt{p_1^*}\,,\ \delta = k_{z\delta} z\,, \tag{31}$$

$$Q_{eng} = Q_{eng}(n)\,, \tag{32}$$

μ_f – exhaust flaps' flow rate co-efficient; l_f, r_f – exhaust flaps' geometry; δ – exhaust flaps' opening.

The non-linear system's mathematical model is built of Eq. (12) to Eq. (32), but it is difficult to be used for study under this form.

3.2. Linearised Mathematical Model

The above determined non-linear equation system can be linearised using the small perturbation method, considering formally any variable X as $X = X_0 + \Delta X$ and $\overline{X} = \frac{\Delta X}{X_0}$, where ΔX – deviation, X_0 – steady state regime's value and $\overline{X}$ – non-dimensional deviation.

Supplementary, some hypothesis can be made, considering that the system works nearby an equilibrium position $V_{A0} \approx V_{B0} = V_1$, $V_{C0} \approx V_{D0} = V_2$, $p_{A0} \approx p_{B0} = \frac{p_a - p_e}{2} = p_{C0} \approx p_{D0}$, $p_{R0} = p_{10}^* + \frac{k_1 x_0}{S_m}$.

Consequently, one obtains

$$l_1 \Delta p_m^* - l_2 \Delta p_m = \frac{k_{r1} l_1 + k_{r2} l_2}{S_a} \left(T_x^2 \frac{\mathrm{d}^2}{\mathrm{d}t^2} \Delta x + 2T_x \omega_0 \frac{\mathrm{d}}{\mathrm{d}t} \Delta x + \Delta x \right), \tag{33}$$

$$\beta_{hf} V_1 \frac{\mathrm{d}}{\mathrm{d}t} (\Delta p_A - \Delta p_B) + k_{Ap} (\Delta p_A - \Delta p_B) = = 2k_{Ax} \Delta x - 2S_p \frac{\mathrm{d}}{\mathrm{d}t} \Delta y\,, \tag{34}$$

$$\Delta p_A - \Delta p_B = \frac{k_{ea}}{S_p} \left(T_y^2 \frac{\mathrm{d}^2}{\mathrm{d}t^2} \Delta y + 2T_y \omega_0 \frac{\mathrm{d}}{\mathrm{d}t} \Delta y + \Delta y \right), \tag{35}$$

$$k_m \Delta p_m^* - (k_m + k_{RH}) \Delta p_R = S_R \frac{\mathrm{d}}{\mathrm{d}t} \Delta w + \beta_{hf} V_R \frac{\mathrm{d}}{\mathrm{d}t} \Delta p_R\,, \tag{36}$$

$$\Delta p_R - \Delta p_1^* = \frac{k_1}{S_R} \left(T_w^2 \frac{\mathrm{d}^2}{\mathrm{d}t^2} \Delta w + 2T_w \omega_0 \frac{\mathrm{d}}{\mathrm{d}t} \Delta w + \Delta w \right) \tag{37}$$

$$\beta_{hf} V_2 \frac{\mathrm{d}}{\mathrm{d}t} (\Delta p_C - \Delta p_D) + k_{pp} (\Delta p_C - \Delta p_D) = = 2k_w \Delta w - 2S_R \frac{\mathrm{d}}{\mathrm{d}t} \Delta z\,, \tag{38}$$

$$\Delta p_C - \Delta p_D = \frac{k_2}{S_p} \left(T_z^2 \frac{\mathrm{d}^2}{\mathrm{d}t^2} \Delta z + 2T_z \omega_0 \frac{\mathrm{d}}{\mathrm{d}t} \Delta z + \Delta z \right), \tag{39}$$

$$\Delta \delta = k_{z\delta} \Delta z\,, \tag{40}$$

$$k_{Qn} \Delta p_m^* = k_{Q1} \Delta p_1^* + k_{Q\delta} \Delta \delta + k_{Qn} \Delta n\,, \tag{41}$$

where $k_{Ax} = \mu_a L_d \sqrt{\frac{p_a - p_e}{\rho_{hf}}}$, $T_x = \sqrt{\frac{m l_2 l_4}{(k_{r1} l_1 + k_{r2} l_2) l_3}}$,

$$2T_x\omega_0=\frac{\xi\, l_2 l_4}{(k_{r1}l_1+k_{r2}l_2)l_3},\ T_y=\sqrt{\frac{m_p}{k_{ea}}},\ 2T_y\omega_0=\frac{\xi_f}{k_{ea}},$$

$$k_{Ap}=\mu_a L_d x_0\sqrt{\frac{1}{\rho_{hf}(p_a-p_e)}},\ T_w=\sqrt{\frac{m_{ra}}{k_1}},$$

$$k_x=\mu_a L_d\sqrt{\frac{p_a-p_e}{\rho_{hf}}},\ T_z=\sqrt{\frac{m_s}{k_2}},$$

$$k_m=\frac{1}{2}\mu_m b L_m\sqrt{\frac{2}{\rho_a}}\frac{1}{\sqrt{p^*_{m0}-p_{R0}}},$$

$$k_{RH}=\frac{1}{2}\mu_{dr}\frac{\pi d_{23}^2}{4}\sqrt{\frac{2}{\rho_a}}\frac{1}{\sqrt{p_{R0}}},\ k_{Qn}=\left(\frac{\partial Q_{eng}}{\partial n}\right)_0,$$

$$k_{pp}=\mu_a L_d w_0\sqrt{\frac{1}{\rho_{hf}(p_a-p_e)}},\ k_{Qm}=KA_m\frac{q(\lambda_m)}{\sqrt{T_1^*}},\quad (42)$$

$$k_{Q1}=\frac{1}{2}\mu_f l_f r_f\delta_0\frac{1}{\sqrt{p^*_{10}}},\ k_{Q\delta}=\mu_f l_f r_f\sqrt{p^*_{10}}.$$

The above presented equations (33) to (41), with the annotation (42), together with the inlet's properties (see (12) and (33)), are building the system's linearised mathematical model.

3.3. Non-Dimensional Linear Model and Block Diagram with Transfer Functions

Applying the Laplace transformation to the above presented (33) to (41) equations and replacing each argument by its non-dimensional deviation, a new form of the system's model shall be obtained.
Noting also

$$k_{xs}=\frac{S_a}{k_{r1}l_1+k_{r2}l_2},\ k_{px}=\frac{2k_{Ax}x_0}{k_{Ap}p_{A0}},\ k_{py}=\frac{S_p p_{A0}}{k_{ea}y_0},$$

$$\tau_{py}=\frac{2S_p y_0}{k_{Ap}p_{A0}},\ \tau_{Ap}=\frac{\beta_{hf}V_1}{k_{Ap}},\ k_{Rw}=\frac{S_R p_{R0}}{k_1 w_0},$$

$$\tau_R=\frac{\beta_{hf}V_2}{k_m+k_{RH}},\ \tau_w=\frac{S_R w_0}{(k_m+k_{RH})p_{R0}},$$

$$\tau_{pw}=\frac{2k_w w_0}{k_{pp}p_{C0}},\ \tau_{pz}=\frac{2S_p z_0}{k_{pp}p_{C0}},\ \tau_{pp}=\frac{\beta_{hf}V_0}{k_p},\ k_{Rz}=\frac{S_p p_{C0}}{k_2 z_0},$$

$$k_{mt}=\frac{l_1 p^*_{m0}}{x_0},\ k_{ms}=\frac{l_2 p_{m0}}{x_0},\ k_{mR}=\frac{k_m p^*_{m0}}{(k_m+k_{RH})p_{R0}},$$

$$k_{m\delta}=\frac{k_{Qm}p^*_{m0}}{k_{Q\delta}\delta_0},\ k_{1\delta}=\frac{k_{Q1}p^*_{10}}{k_{Q\delta}\delta_0},\ k_{n\delta}=\frac{k_{Qn}n_0}{k_{Q\delta}\delta_0},\quad (43)$$

the new form of the mathematical model becomes

$$k_{mt}\overline{p^*_m}-k_{ms}\overline{p_m}=\frac{1}{k_{xs}}\left(T_x^2 s^2+2T_x\omega_0 s+1\right)\overline{x},\quad (44)$$

$$\left(\tau_{Ap}s+1\right)\left(\overline{p_A}-\overline{p_B}\right)=k_{px}\overline{x}-\tau_{py}s\overline{y},\quad (45)$$

$$\overline{p_A}-\overline{p_B}=\frac{1}{k_{py}}\left(T_y^2 s^2+2T_y\omega_0 s+1\right)\overline{y},\quad (46)$$

$$k_{mR}\overline{p^*_m}-\left(\tau_R s+1\right)\overline{p_R}=\tau_w s\overline{w},\quad (47)$$

$$\overline{p_R}-\overline{p_1^*}=\frac{1}{k_{Rw}}\left(T_w^2 s^2+2T_w\omega_0 s+1\right)\overline{w},\quad (48)$$

$$\left(\tau_{pp}s+1\right)\left(\overline{p_C}-\overline{p_D}\right)=k_{pw}\overline{w}-\tau_{pz}s\overline{z},\quad (49)$$

$$\overline{p_C}-\overline{p_D}=\frac{1}{k_{Rz}}\left(T_z^2 s^2+2T_z\omega_0 s+1\right)\overline{z},\quad (50)$$

$$\overline{p_1^*}=k_{m1}\overline{p^*_m}-k_{1\delta}\overline{\delta}-k_{np}\overline{n},\quad (51)$$

$$\overline{\delta}=k_\delta\overline{z}.\quad (52)$$

The above presented equations, together with the inlet's equations

$$\overline{p^*_m}=k_{Hm}\overline{M_H};\ \overline{p_m}=k_{Hs}\overline{M_H}+k_{ns}\overline{n},\quad (53)$$

are representing the system's linear non-dimensional mathematical model; the system's block diagram with transfer functions (based on its linearised equations) is shown in fig. 6.

3.4. Simplified Mathematical Model

Analysing the equation system, as well as the block diagram in fig. 6, one can observe that the main sub-systems are clearly "insulated", each one of them could be described by its own transfer function and its own block diagram (as shown in [14] and [15]).
The connection between the control systems is

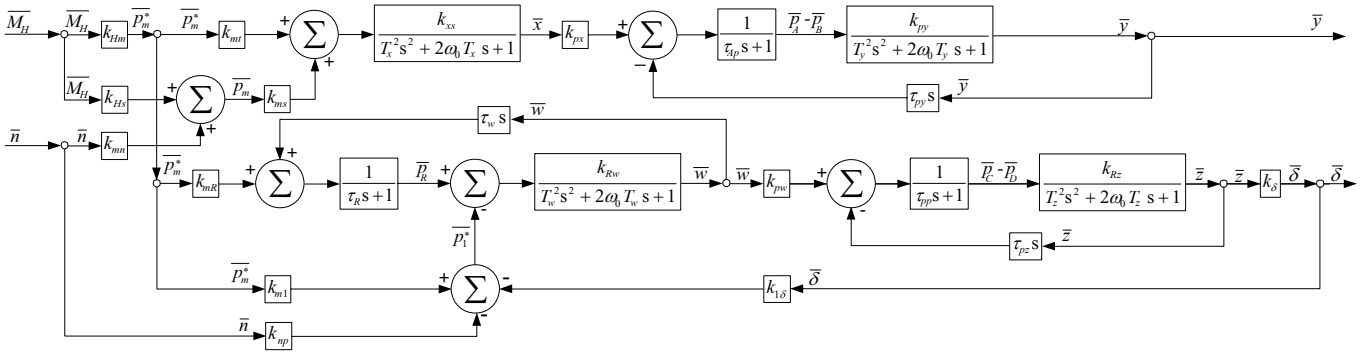

Fig. 6. System's block diagram with transfer functions

given by the input signal forming methods (more precisely: the coupling between the flight regime M_H input and the engine's regime *n* input).

Each model and each transfer function can be simplified if one assume some new hypothesis, as follows: 1) the inertial effects are very small, because of the reduced masses *m*, m_p, m_p and m_{ra} so the time constants T_x, T_y, T_w and T_z can be considered null; 2) viscous friction effects can also be neglected, so the terms containing ξ_f or ξ as multipliers become null; 3) hydraulic fluid's compressibility is practically null, so the terms where β_{hf} is involved become also null (see $\tau_{Ap}, \tau_R, \tau_{pp}$).

Consequently, the new, simplified, form of the system's linear non-dimensional mathematical model

becomes

$$\bar{x} = k_{xs}\left(k_{mt}\,\overline{p_m^*} - k_{ms}\,\overline{p_m}\right), \tag{54}$$

$$\overline{p_A} - \overline{p_B} = k_{px}\bar{x} - \tau_{py}\mathrm{s}\bar{y}\,, \tag{55}$$

$$\bar{y} = k_{py}\left(\overline{p_A} - \overline{p_B}\right), \tag{56}$$

$$k_{mR}\,\overline{p_m^*} - \overline{p_R} = \tau_w \mathrm{s}\bar{w}\,, \tag{57}$$

$$\bar{w} = k_{Rw}\left(\overline{p_R} - \overline{p_1^*}\right), \tag{58}$$

$$\overline{p_C} - \overline{p_D} = k_{pw}\bar{w} - \tau_{pz}\mathrm{s}\bar{z}\,, \tag{59}$$

$$\bar{z} = k_{Rz}\left(\overline{p_C} - \overline{p_D}\right), \tag{60}$$

$$\overline{p_1^*} = k_{m1}\,\overline{p_m^*} - k_{1\delta}\bar{\delta} - k_{np}\bar{n}\,, \tag{61}$$

$$\bar{\delta} = k_\delta \bar{z}\,. \tag{62}$$

$$\overline{p_m^*} = k_{Hm}\overline{M_H};\ \overline{p_m} = k_{Hs}\overline{M_H} + k_{ns}\bar{n}\,. \tag{63}$$

The simplified block diagram with transfer functions, based on the above determined simplified mathematical model equations, is presented in fig. 7, which is offering a simplified system approach possibility.

4. About System's Quality

Based on the above-presented mathematical model and block diagrams with transfer functions, some simulations were performed, in order to study the system's quality, concerning the system's behavior, as its response for step input of the flight regime and of the engine's operating regime.

The values used for the co-efficient are the common values for nowadays operating systems (actuators, sensors etc, as presented in [10], [13] and [12]).

The simulations were performed for 3 situations: a) step input of the flight regime (flight Mach number), engine constant regime; b) step input of the engine operating regime (speed), constant flight regime; c) step input of both engine operating regime and flight regime.

System's step response for the above mentioned cases is presented by the diagrams in fig. 8 a), b) and 9, concerning the diaphragm positioning (*y*) and the exhaust flaps opening (δ).

Some observations can be made, concerning the system's quality and stability. So, in all of the studied cases, the system is a stabile one for both of the studied parameters (*y* and δ), its stability being a non-periodical one, as all the curves in fig. 8 show.

The system is affected by static errors, which means that the new positions of the controlled elements (diaphragm and flaps) have deviations from the imposed values. Although, the positioning errors are acceptable; more precisely: the error values are under 3% (which is an appropriate value for this kind of systems).

Practically, the step input for the flight regime

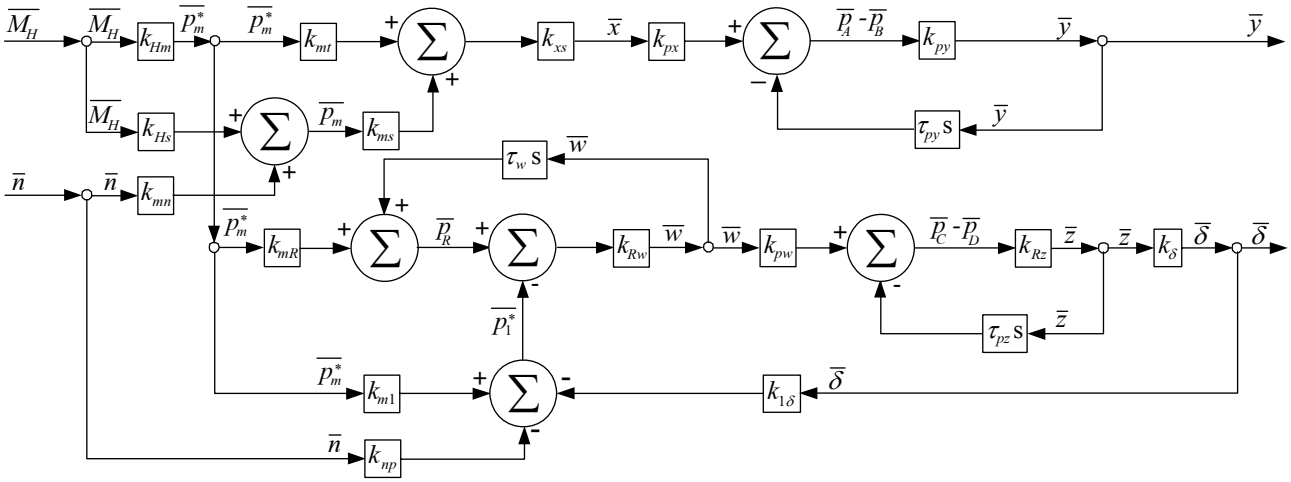

Fig. 7. System's simplified block diagram with transfer functions

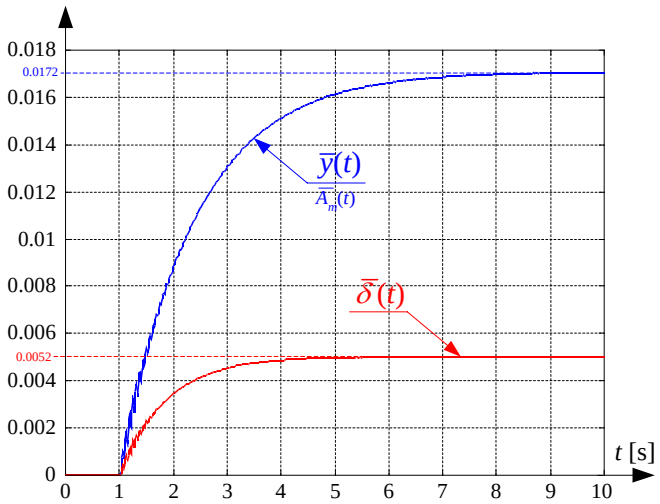

a) system's response for step input of engine operating regime and constant flight regime

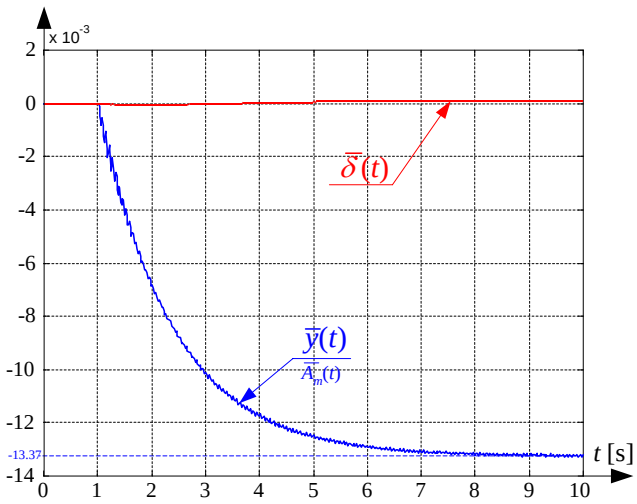

b) system's response for step input of flight regime and constant engine operating regime

Fig. 8. System's time behavior, for different input parameters

doesn't activate the normal shock waves positioning system, which is shown in fig. 8.b), where the flaps opening is nearly null (or insignificantly small). The shock wave positioning system becomes active when the engine's operating regime changes.
Fig. 9 shows the system's time response for both step inputs (Mach number and engine's speed).

5. Conclusions

The authors have studied a dual control system for a supersonic inlet, starting from the motion equation. A mathematical model was issued and, based on it, some computer simulation, concerning its time behavior, were also performed.

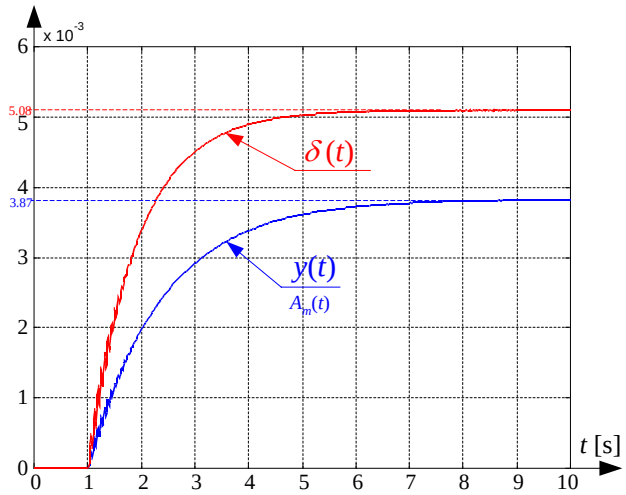

Fig. 9. System's time behavior (step input of both flight regime and engine operating regime)

This complex control system is a combination of two control systems, which can operate each one independently. Although, the new system has specific properties, some of them depending on the parts properties, but also some brand new properties, as consequence of the sub-systems inter-operability (each one loosing its autonomy because of the gas-dynamic coupling).
As far as the inner normal shock wave is kept behind the minimum section of the channel (supersonic regimes, close enough to the nominal regime), the sub-system controlling its position has no influence above the other sub-system, that because of the lack of influence of the flow behind the shock wave above the Mach number before the shock wave, in the minimum section. If the normal shock wave is evacuated until the front of the air intake or it disappears (low speed supersonic regimes, or transonic regimes), its control sub-system becomes inactive, which means a restraint of the control scheme and of the control possibilities.
Obviously, if the exhaust flaps opening angle is modified, the inner normal shock wave's position with respect to the intake's edge changes too, but this repositioning doesn't modify the Mach number in the minimum section.
One can affirm that the system which controls the diaphragm position is more important, that because the repositioning of the minimum section modifies the gas-dynamic distribution in the inlet's channel in any situation and, consequently, the repositioning of the inner normal shock wave, which activates the second control sub-system (see curves in fig. 8.a). Consequently, the system cannot realize the minimum section control without the normal shock

wave's position control, which gives a supplementary error.

Comparing the corresponding curves in fig. 8.a), 8.b) and 9, one can observe that the system is more sensible at the flight regime changing, which has a significant influence above both of the external and inner gas-dynamic conditions; in the mean time, the inlet's inner gas-dynamic behavior is controlled by the shock-wave's positioning, so the engine's speed changing is compensated by the exhaust flaps' opening and the excess airflow's evacuation.

The studied system can be used even for the control of a supersonic inlet with external compression (external shock wave system), which has as supplementary gas-dynamic protection an inner supersonic buffer-zone, ended with a normal shock wave. System's mathematical model, the time behavior and the conclusions are very similar, the difference being given by the inlet's gas-dynamic properties.

The supersonic inlets with external compression have a significant advantage above the mixed compression inlets, concerning the "supersonic activation" [11], which means that the external shock wave system activates itself when the flight regime (flight speed before the inlet) reaches the activation value. The mixed compression inlets, as well as the external compression inlets with supersonic buffer zone, need to be assisted during the activation process, that means that their inner flow must be re-configured any time when the external conditions are changing. If this process is not correctly realized, the balance between the engine's necessary airflow and the inlet's available airflow could be rapidly disturbed and some inlet's stall phenomena, as well as engine's compressor's stall phenomena could be induced.

References:

[1] Abraham, R. H. *Complex dynamical systems.* Aerial Press, Santa Cruz, California, 1986.

[2] Aron, I., Tudosie, A., Hydro-mechanical System For The Supersonic Air Inlet's Channel's Section Control, *Proceedings of the International Conference on Applied and Theoretical Electricity*. Craiova, 2000, pp 266-269, ISBN-973-657-005-3.

[3] Coman, A.V., Moldovan, E., A Study of the Frequency Response of Pressure Mechanical Transducer by Using Finite Elements Method, *WSEAS Transactions on Fluid Mechanics*, pp 37-42, Issue 5, Volume 1, May 2006, ISSN 1790-5087.

[4] Krope, J., Dobersek, D., Goricanec, D., Variation of Pipe Diameters and its Influence on the Flow-Pressure Conditions, *WSEAS Transactions on Fluid Mechanics*, pp 53-58, Issue 1, Volume 1, January 2006, ISSN 1790-5087.

[5] Lungu, R. *Flight apparatus automation.* Publisher Universitaria, Craiova, 2000.

[6] Mattingly, J. D. *Elements of gas turbine propulsion.* McGraw-Hill, New York, 1996.

[7] Mohammad, A. J., A Numerical Study of Shock Reflection Phenomena in Shock/Turbulence Interaction *WSEAS Transactions on Fluid Mechanics*, pp 967-972, Issue 11, Volume 1, November 2006, ISSN 1790-5087.

[8] Pekar, L., Prokop, R., Control of Delayed Integrating Process Using Two Feedback, *Proceedings of the 7th WSEAS International Conference on System Science and Simulation in Engineering (ICOSSE'08)*,pp. 35-40, ISSN 1790-2769, ISBN 978-960-474-027-7

[9] Stevens, B.L., Lewis, E. *Aircraft control and simulation*, John Willey Inc. N. York, 1992.

[10] Pimsner, V., Berbente, C. and others *Flows in turbomachinery*, Tehnica Publishing Bucharest, 1996, pp 384. ISBN 973-165-4-17.

[11] Stoenciu, D. *Supersonic inlet's automation.* Publisher of Military Technical Academy in Bucharest, 1984.

[12] Stoicescu, M., Rotaru, C. *Turbo-jet engines. Characteristics and control methods.* Publisher Military Technical Academy, Bucharest, 1999.

[13] Tudosie, A. *Aerospace propulsion systems automation*. Inprint of Univ. of Craiova, 2005.

[14] Tudosie, A. N., Supersonic Air Inlet's Control System Based On The Inner Normal Shock Wave's Position Stabilisation, *Proceedings of the International Conference on Military Technologies ICMT 07*, University of Defense, Brno, 2-4 May 2007, pp 342-349. ISBN: 978-80-7231-238-2.

[15] Tudosie, A. N., Supersonic Air Inlet Control System Based On The Inner Channel Minimum Cross-Section Position Control, *Proceedings of the International Conference on Military Technologies ICMT 09*, University of Defense, Brno, 5-7 May 2009, pp 350-359. ISBN: 978-80-7231-648-9/ SBN 978-80-7231-649-6.